Article

SOURCE DATA | TRANSPARENT PROCESS

THE EMBO JOURNAL

NTR1 is required for transcription elongation checkpoints at alternative exons in *Arabidopsis*

Jakub Dolata[1,†], Yanwu Guo[2,†,*], Agnieszka Kołowerzo[3,4], Dariusz Smoliński[3,4], Grzegorz Brzyżek[2], Artur Jarmołowski[1] & Szymon Świeżewski[2,**]

Abstract

The interconnection between transcription and splicing is a subject of intense study. We report that *Arabidopsis* homologue of spliceosome disassembly factor NTR1 is required for correct expression and splicing of *DOG1*, a regulator of seed dormancy. Global splicing analysis in *atntr1* mutants revealed a bias for downstream 5′ and 3′ splice site selection and an enhanced rate of exon skipping. A local reduction in PolII occupancy at misspliced exons and introns in *atntr1* mutants suggests that directionality in splice site selection is a manifestation of fast PolII elongation kinetics. In agreement with this model, we found AtNTR1 to bind target genes and co-localise with PolII. A minigene analysis further confirmed that strong alternative splice sites constitute an AtNTR1-dependent transcriptional roadblock. Plants deficient in PolII endonucleolytic cleavage showed opposite effects for splice site choice and PolII occupancy compared to *atntr1* mutants, and inhibition of PolII elongation or endonucleolytic cleavage in *atntr1* mutant resulted in partial reversal of splicing defects. We propose that AtNTR1 is part of a transcription elongation checkpoint at alternative exons in *Arabidopsis*.

Keywords alternative splicing; elongation checkpoint; transcription
Subject Categories Chromatin, Epigenetics, Genomics & Functional Genomics; Plant Biology; Transcription
DOI 10.15252/embj.201489478 | Received 31 July 2014 | Revised 7 October 2014 | Accepted 12 November 2014 | Published online 7 January 2015
The EMBO Journal (2015) 34: 544–558

Introduction

Splicing is a highly complicated process that involves more than 200 proteins and five small RNAs associated with the spliceosome at different stages of splicing (Wahl *et al*, 2009). This enormous number of proteins is reflected in the number of molecular processes, including transcription, that are intertwined with splicing. Alternative splicing is a manifestation of this vast complexity, with more than 95% of human and 60% of *Arabidopsis* genes showing at least two splicing isoforms (Pan *et al*, 2008; Filichkin *et al*, 2009; Marquez *et al*, 2012).

One of the key plant developmental regulators with reported alternative splicing of its pre-mRNA is the DELAY OF GERMINATION 1 protein, DOG1 (Bentsink *et al*, 2006). The *DOG1* expression level is responsible for the delay of germination in freshly harvested seeds and is regulated by various transcription elongation factors (Liu *et al*, 2007; Grasser *et al*, 2009), making it a good plant model for studying the crosstalk between splicing and elongation.

The interconnection of transcription and splicing has been extensively studied (Howe *et al*, 2003; Pagani *et al*, 2003; Chanarat *et al*, 2011; Close *et al*, 2012). Several models have been proposed to explain how chromatin regulates alternative splicing, including the direct sensing of histone modifications by spliceosome-associated factors, and influence of the transcription elongation rate on alternative splice site selection. This latter model is known as the kinetic coupling model (De la Mata *et al*, 2003). It is based on the observation that the changes of RNA polymerase II (PolII) elongation rate affect the selection of alternative splice sites: the slowing down of polymerase leads to exon inclusion and upstream splice site selection, while the acceleration of PolII leads to exon skipping and downstream splice site selection. Recent splicing analysis of a broad list of yeast PolII mutants, with slow and fast elongation kinetics, has confirmed the original model (Braberg *et al*, 2013). Although the slow PolII leads mainly to exon inclusion, there are several reports where reduced PolII elongation results in increased alternative exon skipping, including exon 9 of *CFTR* gene (Dutertre *et al*, 2010; Ip *et al*, 2011; Dujardin *et al*, 2014). For this gene, the slow elongation facilitates the binding of a negative regulator to nascent RNA that in turn results in exon skipping rather than exon inclusion (Dujardin *et al*, 2014).

Genetic analyses have suggested that *DOG1* is a direct target of TFIIS (Mortensen & Grasser, 2014). TFIIS is an elongation factor (Sekimizu *et al*, 1976) required for RNA polymerase II processivity both *in vitro* (Izban & Luse, 1992; Reines, 1992; Cheung & Cramer,

1 Department of Gene Expression, Institute of Molecular Biology and Biotechnology, Adam Mickiewicz University, Poznań, Poland
2 Department of Protein Biosynthesis, Institute of Biochemistry and Biophysics, Polish Academy of Sciences, Warsaw, Poland
3 Department of Cell Biology, Faculty of Biology and Environment Protection, Toruń, Poland
4 Centre for Modern Interdisciplinary Technologies, Nicolaus Copernicus University, Toruń, Poland
*Corresponding author. Tel: +48 22 5925722; E-mail: goanve@gmail.com
**Corresponding author. Tel: +48 22 5925725; E-mail: szymon.swiezewski@gmail.com
†These authors contributed equally to this work

2011) and *in vivo* (Sigurdsson *et al*, 2010). In agreement with the kinetic coupling model, *tfIIs* mutant shows defects in splicing of a reporter gene in yeast (Howe *et al*, 2003).

In addition, transient, splicing-dependent hyper-accumulation of a paused polymerase at the intron was visualised in yeast by the use of synchronised reporter system (Alexander *et al*, 2010). This transient transcriptional pausing event was suggested to constitute a quality checkpoint imposed by co-transcriptional splicing. This interpretation is consistent with the observed over-accumulation of PolII in humans at alternative introns and exons (Batsché *et al*, 2005; Saint-André *et al*, 2011).

NTR1 is an accessory spliceosomal component that has been characterised as an interactor of the NineTeen Complex (NTC) in yeast (Tsai, 2005; Agafonov *et al*, 2011). NTR1 increases PRP43 helicase activity, facilitating intron lariat release. In addition, NTR1 has been proposed to assist in the PRP43-dependent spliceosome quality checkpoint throughout the splicing cycle (Koodathingal *et al*, 2010; Mayas *et al*, 2010). In agreement with this, NTR1 has been repeatedly co-purified with the spliceosome at different stages of splicing (Cvitkovic & Jurica, 2013).

The spliceosome complex has not been purified in plants, but the *Arabidopsis* SPLICEOSOMAL TIMEKEEPER LOCUS 1 protein (STIPL1) has been characterised as a homologue of NTR1 (Jones *et al*, 2012). In agreement with this interpretation, the mutant of the *Arabidopsis* NTR1 homologue has extensive splicing defects and shows circadian clock defects due to the missplicing of one of the circadian clock genes (Jones *et al*, 2012). Surprisingly, purification of the human NTR1 complex has revealed that, in addition to its interaction with PRP43, it is co-purified with conserved group of proteins containing GCFC domain (GC-rich sequence DNA-binding factor): C2ORF3 and GCFC (Yoshimoto *et al*, 2014). The closest *Arabidopsis* homologue of C2ORF3 and GCFC is ILP1, a protein shown to bind DNA and to control endoreduplication (Yoshizumi *et al*, 2006).

Here, we report that the *Arabidopsis thaliana* NTR1 homologue (AtNTR1) is crucial for *DOG1* expression and splicing. Analysis of splicing defects of *DOG1* and other genes shows a strong bias towards downstream splice site selection in *atntr1*. In accordance with kinetic coupling model, we hypothesise that this bias is a consequence of fast PolII elongation at the splice sites in *atntr1* mutant. Our PolII ChIP data revealed localised decrease in PolII occupancy at affected splice sites. This result is interpreted by us as a localised change in elongation rate. We were unable to reproduce this phenomenon using neither chemical modulation of splicing, nor mutants in other splicing factors, which proves that localised decrease in PolII occupancy is AtNTR1-specific. This interpretation is consistent with observed immuno-co-localisation of AtNTR1 with PolII in the nucleus and the presence of AtNTR1 at DNA of its target genes as shown by ChIP. Analysis of AtNTR1-dependent splicing events showed that NTR1 is required for splicing of strong, consensus-like, alternative splice sites. This was corroborated by mutational analysis that showed an *atntr1*-dependent increased accumulation of PolII ChIP signal at the strong alternative splice sites. Our data are consistent with NTR1 being required for co-transcriptional pausing of polymerase at strong alternative splice sites. We therefore interpret the directionality of alternative splicing defects in *atntr1* mutant as a manifestation of PolII elongation defects.

The role of transcription elongation in alternative splice site selection has been extensively studied (De la Mata *et al*, 2011). To investigate whether alternative splice site selection in plants also depends on transcription elongation rate, we have compromised PolII elongation by mutating TFIIS and exposed plants to 6AU (6-azauracil) and MPA (mycophenolic acid) treatment. Observed changes in alternative splicing were predominantly opposite to ones observed in *atntr1* mutant and consistent with prediction based on the kinetic coupling model, supporting our conclusions.

Results

AtNTR1 regulates seed dormancy, *DOG1* expression and splicing

The NTR1 homologue in *Arabidopsis* was originally identified by means of genetic screen aimed to identify circadian clock regulators (Jones *et al*, 2012). We found that in addition to its role in circadian clock regulation, *atntr1-1* mutants showed pleiotropic phenotypes including low seed dormancy, altered flowering time, altered leaf morphology and enhanced lethality at elevated temperatures (Fig 1A, Supplementary Fig S1). We focused on the seed dormancy phenotype and confirmed that both the available alleles, *atntr1-1* and *atntr1-2*, showed enhanced germination without stratification (Fig 1A and B, Supplementary Fig S1A). Interestingly, *dog1* mutants have been shown to have similar phenotype (Bentsink *et al*, 2006). In agreement with the low seed dormancy phenotype, we found reduced expression of *DOG1* gene in *atntr1* mutants, both in seeds (Fig 1C) and seedlings (Supplementary Fig S1B). Because AtNTR1 deficiency leads to massive splicing defects in *Arabidopsis* (Jones *et al*, 2012) and *DOG1* is a subject of alternative splicing (Bentsink *et al*, 2006), we analysed the splicing defects of the *DOG1* transcripts. The *atntr1-1* mutation resulted in more pronounced usage of the 5′ downstream splice site, with a concomitant reduction in the upstream 5′SS selection in comparison with wild-type plants (Fig 1D). Additionally, an approximately 50% increase in intron retention was observed (Fig 1D). The altered splicing isoforms corresponded to the most abundant splice isoforms of *DOG1*, namely alpha and beta (Bentsink *et al*, 2006; Schwab, 2008). Consequently, we have measured all four isoforms reported for *DOG1* and found that, indeed, isoforms alpha and beta were the most affected (Supplementary Fig S1C and D).

The *atntr1* mutant shows bias in alternative 5′ and 3′ splice site selection

We were intrigued by the change in splice site selection on *DOG1* towards the downstream splice site. *DOG1* expression strongly depends on factors required for efficient transcription elongation (including TFIIS). The observed tendency towards downstream splice site selection in the NTR1 mutant could be a manifestation of a defect in the PolII elongation rate (Liu *et al*, 2007; Mortensen & Grasser, 2014). We therefore extended our observation of alternative splicing changes. Independently of the previous report, a selection of 144 alternative splice events were analysed in *atntr1-1* and in wild-type plants (Jones *et al*, 2012). In agreement

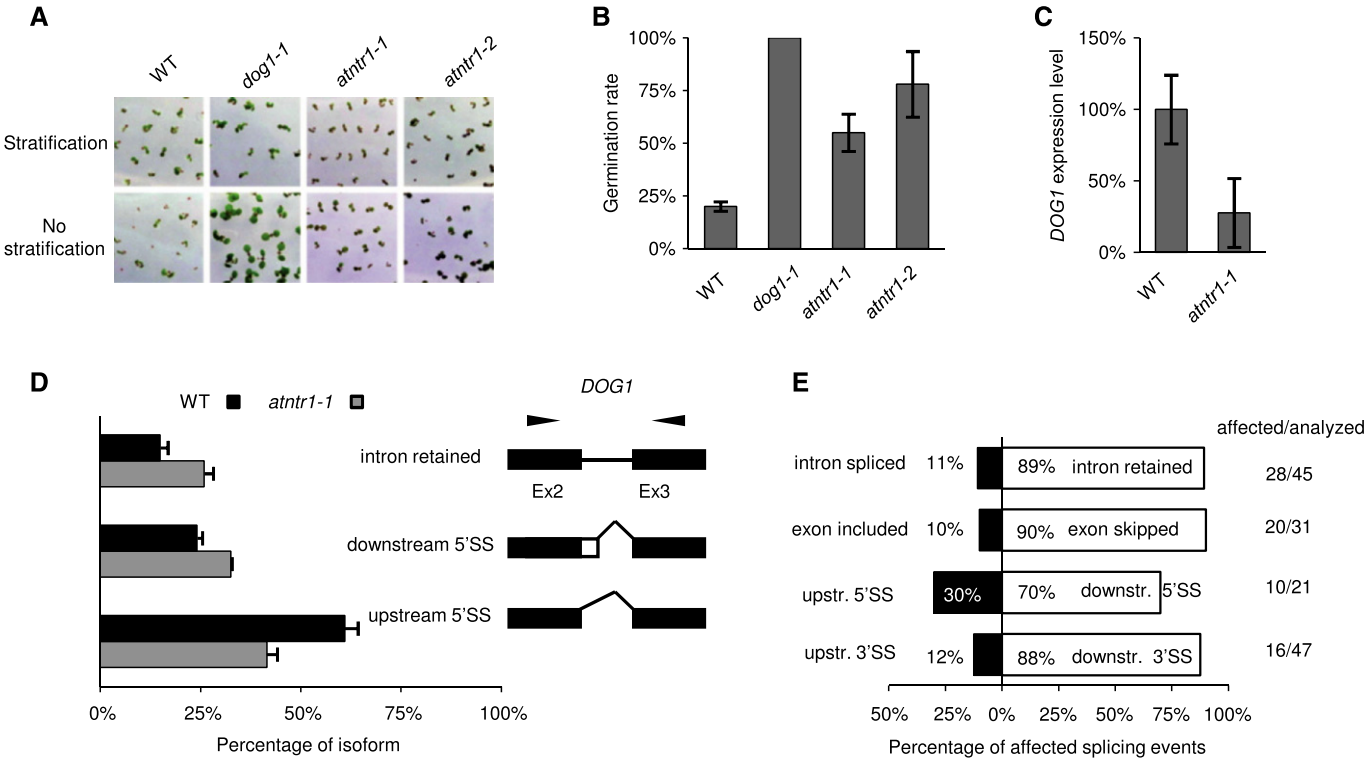

Figure 1. AtNTR1 mutation results in reduced seed dormancy, low *DOG1* expression and a tendency towards downstream splice site selection.

A, B Photographs (A) and quantification (B) of seed dormancy tests. The chart represents the average percentage of germinated seeds without stratification after 4 days of growth in LD. The error bars represent ± SE (n = 3). Tests were performed on freshly harvested seeds, with or without 3 days of stratification growth in LD.

C qPCR of *DOG1* expression in siliques (16 days after pollination). The graph represents the average ratio of *DOG1* to *UBC*, normalised to Col-0 (WT). The error bars represent ± SE (n = 3).

D *DOG1* splicing was assessed by RT–PCR combined with capillary electrophoresis. The graph represents the mean relative contribution of the mRNA forms found in the total pool of amplified products. The black and grey bars represent the data for Col-0 and *atntr1-1*, respectively. The error bars represent ± SD (n = 3). To the right of the charts, the structures of the examined transcripts are shown (black boxes, constitutive exons; white boxes, alternative regions; black lines, introns). The black arrows show the locations of primers. Downstr. and upstr. stand for downstream and upstream splicing event, respectively.

E Directionality of splice site selection in *atntr1*. Splicing was analysed in 14-day-old MS grown plants. For each type of alternative splice event, the black and white boxes show the contributions of opposite direction splicing events. The numbers represent the percentage of splice events supporting the direction of the splice site event change (also shown on horizontal axis). The numbers on the right-hand panel represent the number of affected splicing events versus total number of splicing events analysed. The white bars represent distal 3′ and downstream 5′ splice site selection (3′SS/5′SS), exon skipping (ES) and intron retention (IR), while the black bars represent 5′ and 3′ splice site selection (3′SS/5′SS), exon inclusion (ES) and intron splicing (IR).

with previous results, we found that the most abundant splicing defects were intron retention and exon skipping (Fig 1E). For 144 alternative splicing events analysed, 74 were significantly changed. Prominent bias in the directionality of alternative 5′ splice site selection was observed, which is in accordance with the directionality of splice site selection on *DOG1* (Fig 1D and E). Of 16 affected alternative 3′ splice site selection events, 14 (88%) were changed in *atntr1-1* towards downstream splice sites (SS). Similar bias was also observed in the directionality of splicing events in the case of 5′ splice site events (seven of 10 changed towards downstream SS—70%) and in exon skipping events (18 of 20 changed towards exon skipping—90%) (Fig 1E and Supplementary Table S1).

Upstream/downstream splice site selection has been proposed to represent a manifestation of the polymerase II elongation rate (De la Mata *et al*, 2003, 2011). Consequently, the observed bias could indicate a defect in transcription elongation across the affected splice sites in the *atntr1-1* mutant.

AtNTR1 is required for splicing of strong consensus splice sites

Next, we wanted to understand what creates specificity for AtNTR1 at some splice sites but not the others. Analysis of acceptor splice sites sequences showed no clear difference between AtNTR1-dependent and AtNTR1-independent introns (Supplementary Fig S2B). On the other hand, analysis of donor sites revealed a significant difference at position+3/+4 (P-value < 0.05, Fisher's exact test). AtNTR1-dependent introns show a higher likelihood of A/G at +3 and A at +4 positions compared to AtNTR1-independent splice sites (Supplementary Fig S2A). The consensus donor splicing site sequence in *Arabidopsis* is AG|GTAAGT. Consequently, the affected introns more closely resemble the whole-genome consensus than introns with splicing unaffected in *atntr1-1*.

We decided to test whether the AtNTR1 requirement for splicing is specified by the strong sequence of alternative splicing donor splice site as has been suggested by our sequence analysis. We selected an alternative 5′SS event that is not dependent on NTR1

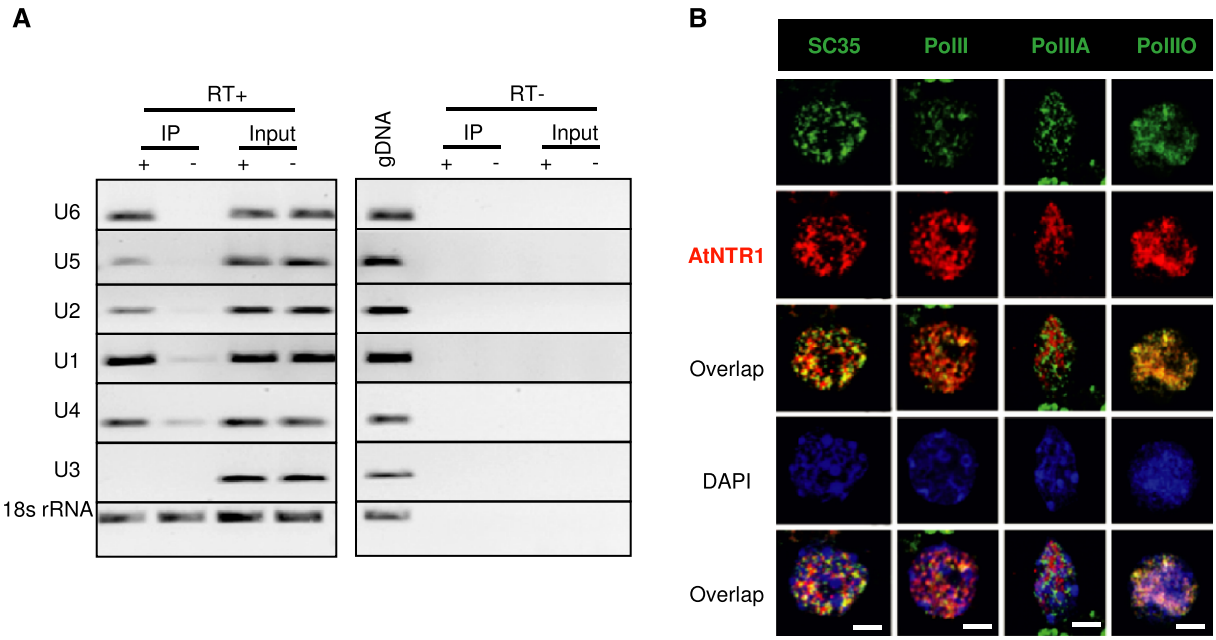

Figure 2. AtNTR1 interacts with U6 and U1 snRNA and co-localise with PolII.

A Electrophoresis of RT–PCR products showing interactions of AtNTR1 with selected snRNA targets detected by RIP. The level of transcripts co-precipitated from transgenic plants expressing ANTR1-GFP (IP+) or wild-type plants (IP−) using anti-GFP antibody was measured by RT–PCR normalised to the inputs. To control the amplification from gDNA, controls without reverse transcriptase (RT) were performed. U3 snRNA and 18S rRNA were used as negative controls for interaction.

B Fluorescent immunostaining of nuclei showing the co-localisation of AtNTR1 with SC35, total PolII, Ser5-phosphorylated PolII (PolIIA) or Ser2-phosphorylated PolII (PolIIO). AtNTR1 was detected using an antibody raised against AtNTR1 peptide. Scale bar represents 2.5 μm.

and has week consensus sequences at the upstream and downstream splicing sites. Subsequently, those sites were mutated into strong consensus sequences by changing two nucleotides at each site (Supplementary Fig S1C). Analysis showed that whereas splicing of the native version (5′SS wt) was not changed in *atntr1* mutant, the splicing of the mutated construct (5′SS strong) was affected (Supplementary Fig S1D). Although the change in alternative splice site selection was modest, it was statistically significant (*t*-test *P*-value < 0.01). This confirms our initial observation that the 5′SS consensus with extended homology to U1 constitutes a preferable target for NTR1 splicing activity. In addition, this analysis shows that the AtNTR1 effect on splicing is downstream of splice site recognition by the spliceosome, which is consistent with the AtNTR1 role in recycling of U6.

In addition to U6/5/2 snRNPs, AtNTR1 interacts with U1

To obtain more insights into the potential function of AtNTR1, RNA molecules associated with AtNTR1 were analysed using RNA immunoprecipitation (RIP) followed by RT–PCR. In this experiment, a complementing transgenic *Arabidopsis* line expressing the AtNTR1-GFP fusion protein in the *atntr1-1* genetic background was used with antibodies recognising GFP. Given the well-documented role of NTR1 in U6, U5 and U4 recycling, we tested AtNTR1 interaction with those molecules. We could clearly observe an enrichment of U6, U5 and U2 RNA in the AtNTR1-GFP-immunoprecipitated fraction, compared to our negative control (Fig 2A). Surprisingly, a strong and reproducible interaction of AtNTR1 with U1 was also observed (Fig 2A). In contrast, U3 and 18S rRNA showed no enrichment, confirming the stringency of our method (Fig 2A). This result was further confirmed by the identification of AtNTR1-associated proteins by means of mass spectrometry. The U1 associated protein—U1A—was one of our highest-scoring interactors (Table 1).

ILP1, a GCFC domain-containing protein, interacts with AtNTR1 and is required for efficient splicing

The highest-ranking NTR1 interactor on our list was a protein known as ILP1 in *Arabidopsis* (Yoshizumi *et al*, 2006). ILP1 contains the GCFC domain (GC-rich sequence DNA-binding factor-like domain) and is a homologue of the human proteins C2ORF3 and GCFC (also

Table 1. AtNTR1 co-purifying proteins.

Gene ID	Gene name	MW (Da)	Number of unique peptides P1-P2-P3-P4
AT1G17070	AtNTR1	96,937	37-36-26-30
AT5G08550	ILP1	100,998	21-22-30-28
AT1G24180	IAR4	43,787	1-2-2-2
AT2G39770	CYT1	39,837	1-1-1-2
AT2G47580	U1A	58,456	1-1-1-1
AT2G30050	WD40	32,907	1-1-1-1

Seedlings of complementing AtNTR1-GFP transgenic lines, expressed under native promoter, were used for four independent purifications with three negative controls (Col-0). After trypsin digestion and mass spectrometry, proteins identified in all purifications but not in negative controls were listed in the table. Number of unique peptides matching each identified protein is shown separately for each purification (P1–4).

known as Pax3/7BP) (Diao *et al*, 2012; Yoshimoto *et al*, 2014). Both, the bimolecular fluorescence complementation (BiFC) assay using YFP (Supplementary Fig S3B) and an yeast two-hybrid assay (Supplementary Fig S3C), confirmed our original finding and suggested direct AtNTR1–ILP1 interaction. Interestingly, homologues of ILP1 in human co-purify with TFIP11, a human homologue of AtNTR1 (Yoshimoto *et al*, 2014). This indicates that this interaction is conserved between species, which suggests that it may be important for NTR1 function. ILP1 in *Arabidopsis* binds to a promoter of a key cell cycle gene and controls its expression, providing a possible explanation for endoreduplication defects in the *ilp1* mutant (Yoshizumi *et al*, 2006). In addition, human homologues of ILP1 likewise bind to gene promoters to regulate their expression (Diao *et al*, 2012).

Next, we tested whether ILP1 was involved in splicing regulation in *Arabidopsis*. The *atntr1-1* and *ilp1-1* mutants' analysis revealed that *ilp1-1* had very strong splicing defects, with virtually all splicing events affected in *atntr1-1* also being misregulated in the *ilp1* mutant (Supplementary Fig S3D, Supplementary Table S2). This finding is consistent with the recent data on a human ILP1 homologue showing that the depletion of C2ORF3 by RNAi repressed pre-mRNA splicing in vitro (Yoshimoto *et al*, 2014).

We conclude that ILP1, like its human homologues, is a direct interactor of AtNTR1 and that GCFC domain-containing proteins are required for efficient splicing both in *Arabidopsis* and in humans.

PolII co-localises with AtNTR1

AtNTR1 immunolocalisation was investigated, to test the relationship between AtNTR1 and PolII. We confirmed previous results from human cells showing that NTR1 is localised in the nucleus but excluded from the nucleolus, using a complementing genomic NTR1-GFP line (Supplementary Fig S1I and J) and AtNTR1 antibody (Fig 2B) (Tannukit *et al*, 2008). In addition, it was found that AtNTR1 is only partially co-localised with the SC35 splicing factor using dual labelling (Fig 2B), which is in agreement with results concerning NTR1 mouse homologue (Wen *et al*, 2005). Subsequently, we investigated the co-localisation of AtNTR1 with PolII. Three different PolII antibodies were used: the first recognising all forms of PolII (total PolII), the second recognising the Ser5-phosphorylated form of PolII (PolIIA) that is usually associated with the initiation of transcription, and the third recognising Ser2-phosphorylated PolII (PolIIO), which is believed to primarily mark PolII associated with gene bodies. Partial co-localisation with total PolII was observed. It could be attributed to the Ser2-phosphorylated form of PolII, based on observed no co-localisation with PolIIA and strong co-localisation of AtNTR1 with the PolIIO (Fig 2B). Although the functional distinction between Ser5-phosphorylated and Ser2-phosphorylated PolII is not absolute, it is generally believed that Ser2 phosphorylation is a mark of elongating polymerase (Komarnitsky, 2000; Buratowski, 2009).

AtNTR1 acts co-transcriptionally at affected splice sites

The co-localisation of AtNTR1 with Ser2-phosphorylated PolII suggests that NTR1 can be physically present at the target genes. In order to test this, AtNTR1 localisation on the *DOG1* gene was analysed by chromatin immunoprecipitation (ChIP) using antibodies that recognise AtNTR1.

Our ChIP analysis shows that AtNTR1 is present at the gene body and promoter of *DOG1*, in contrast to an intergenic region selected as a negative control (Fig 3). In addition, a set of five other genes was tested for NTR1 presence. Clear NTR1 signal could be detected on all of them (Supplementary Fig S4). The genes were selected from set that displayed misregulated alternative splicing in *atntr1*. Moreover, the five genes were chosen to represent different types of alternative splicing events. The physical presence of AtNTR1 on those genes substantiates our NTR1 PolII co-localisation data and suggests that at least some of NTR1 activity is happening co-transcriptionally.

We conclude that AtNTR1 is present at or close to DNA of genes that display AtNTR1-dependent splicing. In addition, our ChIP analysis shows that AtNTR1 is present throughout the analysed genes, with no clear enrichment at misspliced introns. This result is consistent with immuno-co-localisation studies of AtNTR1 and PolII.

Localised PolII level reduction in *atntr1* mutant

Our data show a strong link between AtNTR1 and PolII. Moreover, the splicing defects observed in the NTR1 mutant could be a manifestation of fast PolII elongation across these splice sites. We therefore considered a possibility that AtNTR1 is involved in the control of PolII at those splice sites. To address this, the genes that previously showed to be direct AtNTR1 targets were used to assess PolII profile by ChIP using antibodies that recognise total PolII.

Analysis of PolII occupancy in *atntr1-1* consistently revealed a significant reduction in PolII for all genes with AtNTR1-dependent splicing (five of the five genes tested) (Fig 4 and Supplementary Fig S5). With an exception of *DOG1*, the reduction was limited to or strongest at the regions of misspliced introns. The *At5g04430* gene was analysed as a control, as it shows *atntr1*-independent alternative splicing and consequently showed no significant reduction in PolII levels in *atntr1* mutant.

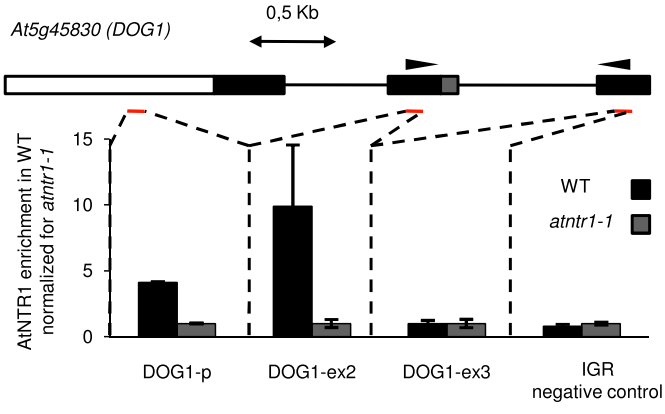

Figure 3. AtNTR1 is present at the *DOG1* gene.
AtNTR1 antibodies were used to analyse AtNTR1 protein presence at *DOG1* locus using ChIP. Data shown represent enrichment above background level measured in *atntr1-1* mutant. Gene structure is shown with black boxes representing constitutive exons; grey box, alternative region; white box, promoter region; black lines, introns. Red lines show amplified regions. 0.5 kb scale is shown. Error bars represent ± SD of three independent experiments. As an additional negative control, primers amplifying an unlinked intergenic region (IGR) were used.

Reduction in PolII levels in *atntr1* is not a consequence of reduced splicing efficiency

Research in yeasts suggests that aberrant splicing may lead to stronger PolII pausing (Alexander *et al*, 2010; Chathoth *et al*, 2014). In the case of *atntr1,* we observe the reduction in PolII accumulation across the intron associated with aberrant splicing. It is possible that the reduction in PolII levels observed in *atntr1* could be a consequence of general splicing malfunction in this mutant. To validate this possibility, we tested whether PolII occupancy defects observed in *atntr1* could be mimicked by alteration of splicing. We first used the chemical modulator of splicing herboxidiene. Herboxidiene is a plant herbicide, which was shown to modulate splicing in humans by direct binding to the spliceosome component SAP155 (Miller-Wideman *et al*, 1992; Hasegawa *et al*, 2011; Lagisetti *et al*, 2014).

Our results show clear alteration of splicing across nearly all analysed splicing events in the case of WT plants treated with herboxidiene (Fig 4, Supplementary Fig S5 and Supplementary Table S3). However, the PolII ChIP occupancy analysis in herboxidiene-treated plants failed to show any significant reduction in PolII levels at the affected splice sites (Fig 4, Supplementary Fig S5). Both herboxidiene and spliceostatin A target the same splicing factor (Kaida *et al*, 2007). That leads to the conclusion that our data are in agreement with data from human studies where spliceostatin A treatment did not cause change in PolII levels or elongation kinetics at the splice sites (Brody *et al*, 2011). Taken together, our results suggest that the reduction in PolII levels in *atntr1* is not a consequence of misregulated splicing but rather a direct affect of NTR1 deficiency.

In addition to chemical modulation of splicing, we tested two splicing mutants known to regulate alternative splicing, namely *sr45-1* and *smd3-b* (Palusa *et al*, 2007; Swaraz *et al*, 2011). Our analysis showed no change in PolII occupancy on any of the six tested genes (Supplementary Fig S6). In contrast, we have found a substantial change in splicing of those genes. These changes were often similar to ones observed for the *atntr1* mutant (Supplementary Fig S6 and Supplementary Table S4). This shows that the PolII occupancy change observed in *atntr1* is not shared among all splicing factor mutants but is specific for the NTR1.

The reduction in PolII level in *atntr1* is unlikely to represent a reduction in overall transcription rate due to the fact that, in majority of cases, it is localised in the vicinity of affected splice sites and cannot be observed throughout the whole gene.

The observed localised decrease in PolII occupancy in *atntr1* mutant could be interpreted in several ways. Given the directionality in splice site selection, we interpret the altered PolII profile as a result of localised change of elongation rate across the affected splice sites. The PolII occupancy analysis in the *atntr1* mutant supports a model, in which the NTR1 facilitates the splice-site-dependent pausing at alternative splice sites in *Arabidopsis*. Alternative splice sites have been shown to accumulate high PolII signal in humans (Saint-André *et al*, 2011). We however could not detect a significant increase in the PolII signal at alternative splice sites when compared to surrounding regions in WT plants, suggesting that there are many parallel mechanisms controlling PolII occupancy at those genes.

AtNTR1 induces pausing of PolII at strong alternative splices sites on the transgene

We previously showed that splicing of our minigene became NTR1 dependent when its sequence was mutated into strong splice site consensus. Next, we wanted to investigate the PolII occupancy using minigenes. To do this, we first analysed transgenic lines with WT alternative 5′ donor splice sites (5′SS wt) and mutated NTR1-dependent strong upstream—strong downstream splice sites (5′SS strong). The 5′SS strong transgene compared to 5′SS wt transgene showed significantly higher PolII levels, specifically at the studied splice site (Fig 5). The 5′SS strong construct differs from the 5′SS wt construct only by 2 nucleotides mutated at upstream and downstream 5′SS, respectively. The dependence of the localised increase in PolII occupancy in our minigene suggests a PolII pause site, controlled by the spliceosome, operates at strong alternative splice sites on our transgene. Localised increase in PolII occupancy is dependent on the presence of strong alternative splice sites. This shows that, in the context of the transgene, the PolII pause site requires strong consensus sequence and suggests PolII pausing is controlled by the spliceosome.

Next we tested whether this PolII pausing on our minigene is NTR1 dependent. Analysis performed in the *atntr1-1* background showed a marked reduction in PolII levels for 5′SS strong but not for the 5′SS wt construct (Fig 5). Those results confirmed that AtNTR1 is required for high PolII occupancy observed on the transgene. We interpret this localised PolII occupancy change as an AtNTR1-dependent transcriptional pausing at strong alternative splice sites of the transgene.

Analysis of endogenous targets in WT plants revealed no substantial increase in PolII occupancy at alternative splice sites compared to surrounding regions. Therefore, we can only speculate that on endogenous genes, similarly to our transgene strong alternative splice sites constitutes a transcriptional pause site, but other PolII elongation control mechanisms mask the result. This interpretation is consistent with the observed reduction in PolII occupancy level observed in *atntr1* mutant at endogenous targets.

The locally increased PolII occupancy, observed at 5′SS strong compared to 5′SS wt construct, together with localised reduction in PolII in *atntr1* both at transgene and endogenous targets, suggests a role of AtNTR1 in transient transcriptional pausing at splice sites. Using chemical or genetic interference, we could not reproduce PolII decrease observed in *atntr1* mutant. Therefore, we interpret the

Figure 4. *atntr1*, in contrast to herboxidiene-treated plants, shows localised decrease in PolII occupancy on alternatively spliced exons.
Line charts present ChIP profile of total PolII on examined genes. Black, grey and dashed black lines represent results for Col-0, *atntr1-1* and herboxidiene-treated WT plants, respectively. Above each chart, gene structure is shown with black boxes representing constitutive exons; grey boxes, alternative regions; white boxes, promoter region; black lines, introns. Red lines show amplified regions. Above each gene structure, 0.5 kb scale is shown. For each chart, the mean value from three independent experiments is shown. Error bars represent ± SD, $^{**}P < 0.01$ and $^{*}P < 0.05$ of *t*-test. Arrows on gene structure show localisation of primers used for splicing analysis by RT-PCR, which was followed by capillary electrophoresis (results shown in tables next to each gene). Tables represent splicing site selection in mutant and herboxidiene-treated plants in comparison with wild-type.
Source data are available online for this figure

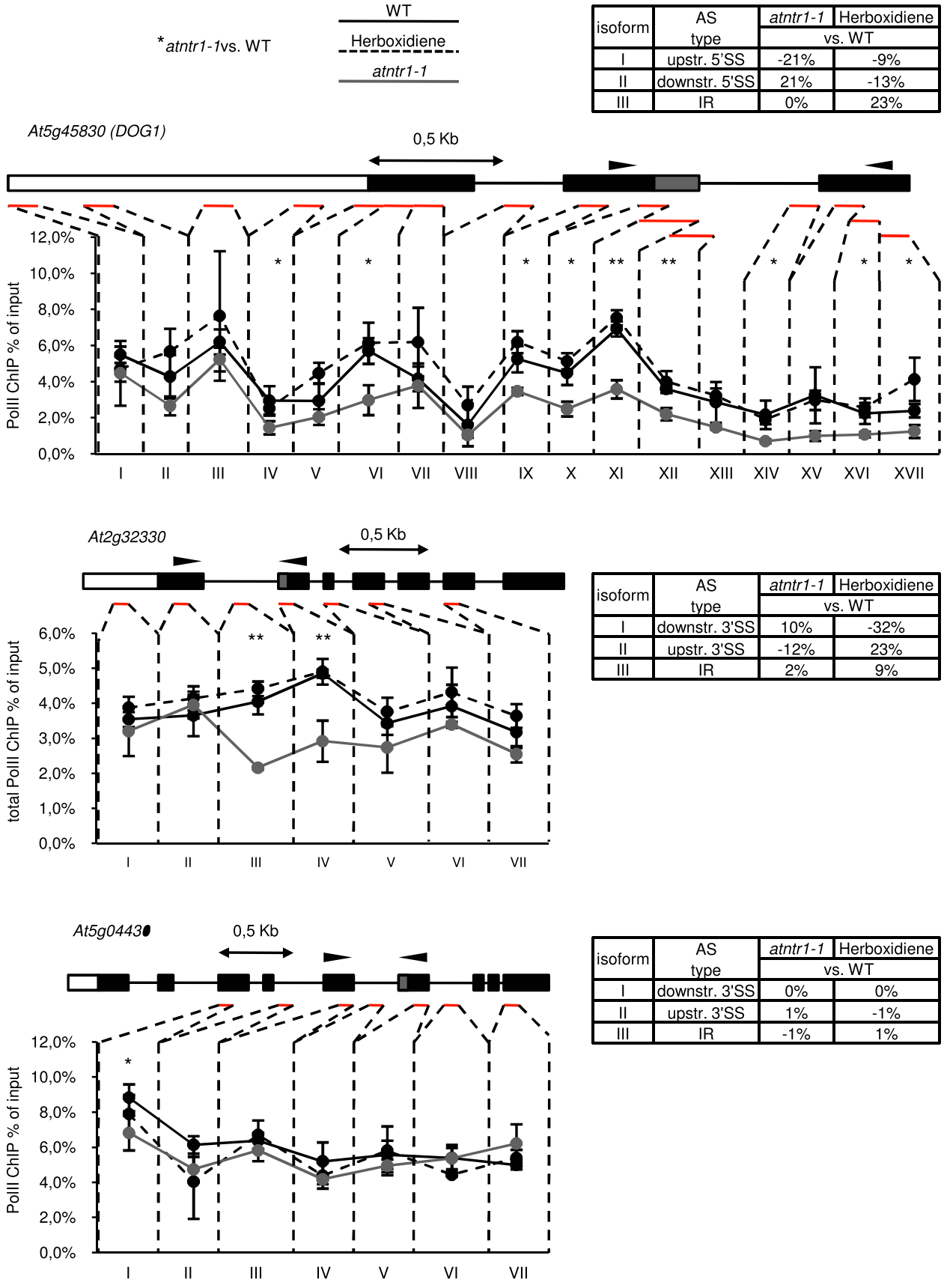

isoform	AS type	*atntr1-1* vs. WT	Herboxidiene vs. WT
I	upstr. 5'SS	-21%	-9%
II	downstr. 5'SS	21%	-13%
III	IR	0%	23%

isoform	AS type	*atntr1-1* vs. WT	Herboxidiene vs. WT
I	downstr. 3'SS	10%	-32%
II	upstr. 3'SS	-12%	23%
III	IR	2%	9%

isoform	AS type	*atntr1-1* vs. WT	Herboxidiene vs. WT
I	downstr. 3'SS	0%	0%
II	upstr. 3'SS	1%	-1%
III	IR	-1%	1%

Figure 4.

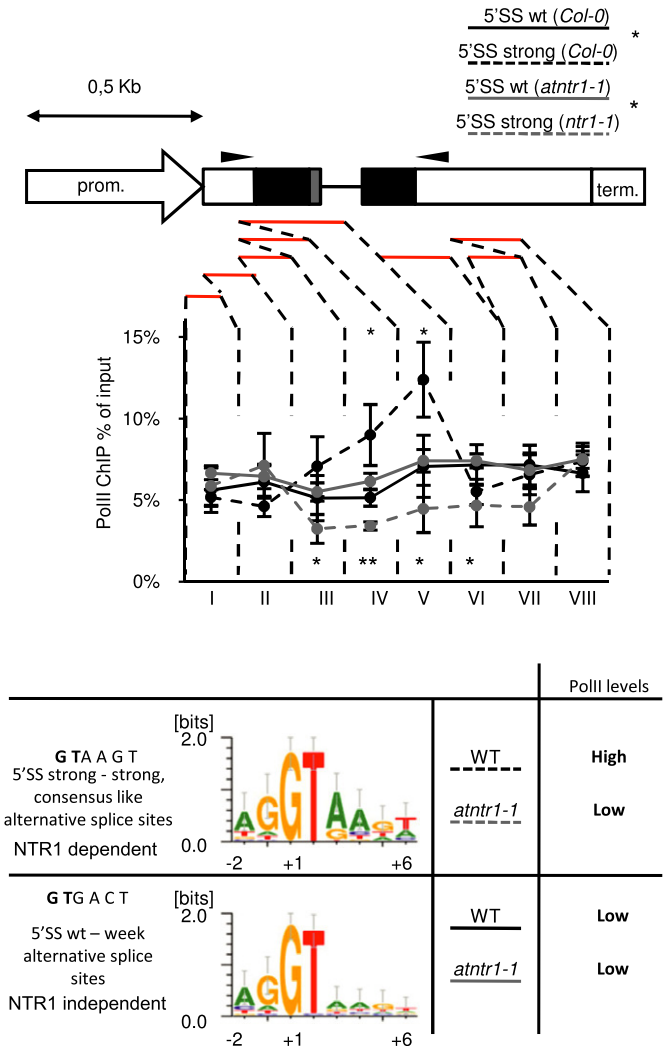

Figure 5. Strong alternative splice sites constitute an AtNTR1-dependent PolII pause site on the minigene.

Transgenic plants expressing 5′SS wt and 5′SS strong constructs were used to perform ChIP experiments using total PolII antibodies. Line charts present ChIP profile of total PolII on minigene. Reporter gene structure is shown with black boxes representing constitutive exons; grey boxes, alternative region; white boxes, promoter and terminator regions; black lines, introns. Red lines show amplified regions. Above gene structure, a 0.5 kb scale is shown. Arrows on gene structure show localisation of primers used for splicing analysis. Error bars represent ± SD of three independent transgenic lines, $^{**}P < 0.01$ and $^{*}P < 0.05$ of *t*-test. Bottom panel shows a schematic representation of 5′SS strong-NTR1-dependent and 5′SS wt-NTR1-independent consensus as described in Materials and Methods.

Source data are available online for this figure

PolII changes detected in *atntr1* not as a consequence of aberrant splicing but rather as a manifestation of AtNTR1 function.

The dominant-negative TFIIS mutant blocking PolII endonucleolytic cleavage shows upstream splice site selection

The directionality of alternative splice site selection and the localised PolII occupancy decrease in *atntr1* are interpreted by us as a consequence of fast PolII elongation in this mutant. It was therefore tested whether in *Arabidopsis*, as in other systems, the reduction in PolII elongation will result in upstream splice site selection and exon inclusion (De la Mata *et al*, 2003; Ip *et al*, 2011). Given that *DOG1*, one of our target genes, has been shown to be regulated directly by TFIIS, we focussed our attention on this mutant (Mortensen & Grasser, 2014). TFIIS is a conserved component of the PolII holoenzyme, required for efficient PolII endonucleolytic cleavage activity (Sigurdsson *et al*, 2010). TFIIS has a modulatory function in the enhancement of PolII processivity, allowing reinitiation of backtracked, paused polymerase. TFIIS mutants have been shown to display splicing defects in yeast and humans (Howe *et al*, 2003; Shukla *et al*, 2011).

We expected that *tfIIs* knockout plants would show enhanced pausing of PolII, which in turn would be reflected in alternative splice site selection. Our splicing analysis in *tfIIs* knockout showed only mild defects in splicing, with 10 of 284 splicing events (including the set analysed for AtNTR1) being affected (Supplementary Fig S7D, Supplementary Table S5). We therefore constructed an enhanced TFIIS mutant in *Arabidopsis* (TFIISmut). To this end, two key amino acids in the TFIIS trigger loop were mutated, as described previously for yeast (Sigurdsson *et al*, 2010) (Supplementary Fig S7A). These mutations result in a protein that not only is unable to activate PolII endonucleolytic cleavage but also blocks it, as was shown in vitro (Sigurdsson *et al*, 2010). We were unable to recover any transformants when TFIISmut construct was expressed the in the *tfIIs* knockout. This suggests that PolII endonucleolytic cleavage is required for the viability of *Arabidopsis*, which is in agreement with findings concerning *Saccharomyces cerevisiae* (Sigurdsson *et al*, 2010). It was however possible to obtain viable transformants when TFIISmut construct was expressed in the WT plants, as in the case of yeast. These transgenic plants showed a range of developmental defects, including leaf serration and reduced steam elongation (Supplementary Fig S7B). We conclude that, similar to *S. cerevisiae*, the TFIISmut protein shows a dominant-negative phenotype.

Next, splicing analysis was repeated in TFIISmut using the same set of splicing events that were analysed for the *tfIIs* knockout. We found that 62 of 284 alternative splicing events were altered (Fig 6, Supplementary Fig S7, Supplementary Table S5). For the majority of these cases, including *DOG1*, preferential selection of the upstream 5′ splice site was observed (nine of 11 cases, Fig 6A and B). In addition, a strong tendency towards enhanced intron splicing in the case of intron retention events (11 of 14) and enhanced exon inclusion in the case of exon skipping (14 of 18 events) was observed (Fig 6B). This type of bias towards upstream splice sites selection, enhanced intron splicing and exon retention has been postulated to result from the kinetic coupling of splicing and transcriptional elongation (De la Mata *et al*, 2003, 2011). In summary, of 62 affected alterative splicing events in TFIISmut, 45 changed in the direction predicted by the kinetic model. Our data do not explicitly prove the existence of kinetic coupling of splicing and transcription elongation in plants, but is consistent with this model.

Most importantly, the directionality of the splice site selection bias in the TFIISmut was predominantly opposite to the changes observed in *atntr1-1* mutant (compare Fig 6B and Fig 1E). A total of 72.5% of the splicing events changed in both TFIISmut and *atntr1* were affected in opposite directions (Fig 6C). These data corroborate our interpretation of directionality in *atntr1* alternative splice site selection as a manifestation of PolII elongation defects.

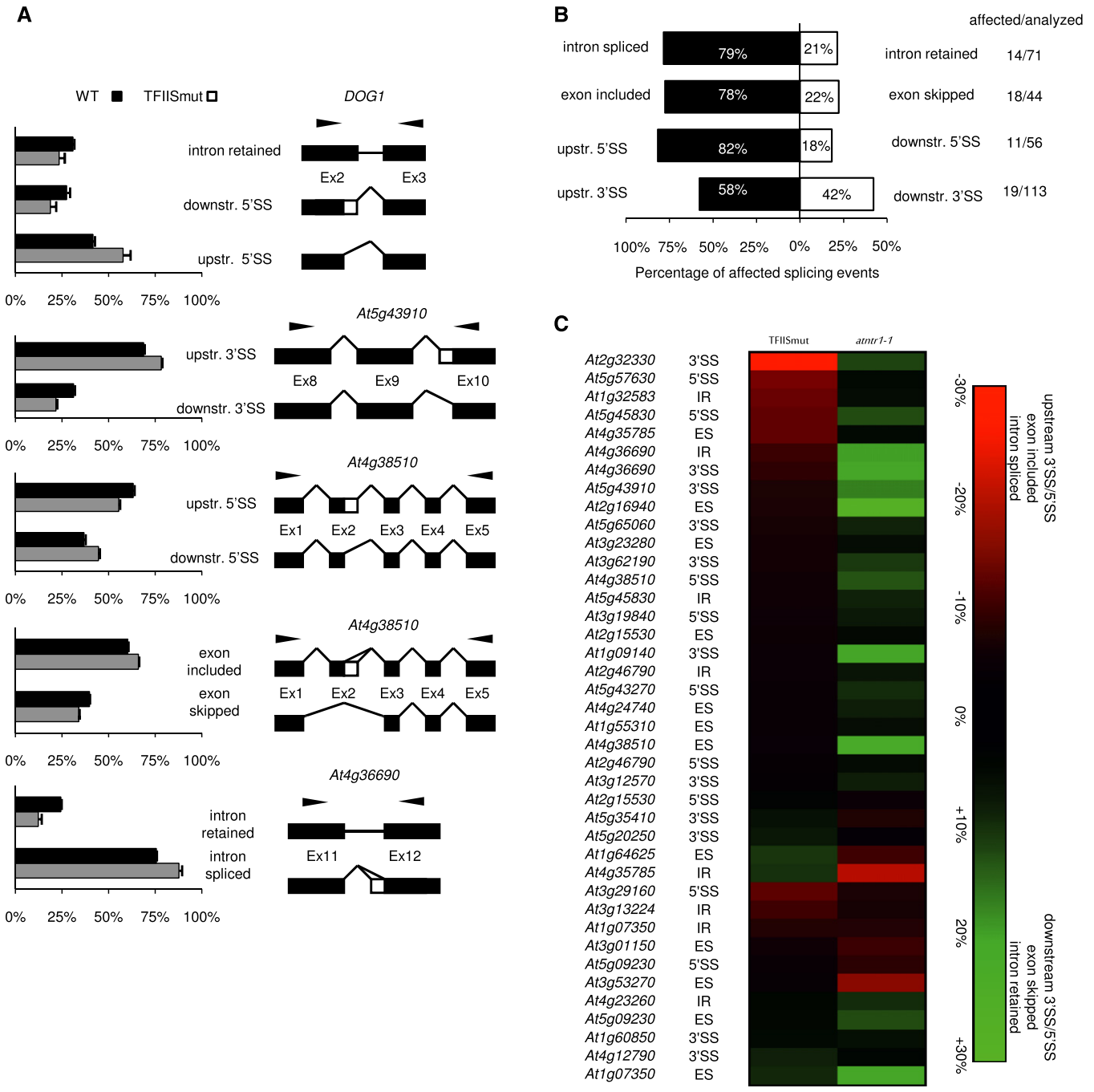

Figure 6. TFIISmut shows splicing defects consistent with kinetic coupling of transcription and splicing.

A TFIISmut shows upstream splice site selection. The splicing was assessed by RT–PCR and capillary electrophoresis in 3-week-old soil grown plants. The chart represents the average relative contribution of the mRNA forms found in the total pool of amplified products. The error bars represent ± SD (n = 3). To the right of the charts, the structures of the examined transcripts are shown. The black boxes, white boxes and black lines represent constitutive exons, alternative regions and introns, respectively. The black arrows show the locations of the primers. Representative splicing assays are shown.

B Directionality of splice site selection in TFIISmut. For each type of alternative splice event, the black and white boxes show the contributions of opposite direction splicing events. The numbers represent the percentage of splice events supporting the direction of the splice site event change (also shown on horizontal axis). The numbers on the right-hand panel represent the number of affected splicing events versus total number of splicing events analysed. The white bars represent downstream 3′ and 5′ splice site selection (3′SS/5′SS), exon skipping (ES) and intron retention (IR), while the black bars represent upstream 3′/5′ splice site selection (3′SS/5′SS), exon inclusion (ES) and intron splicing (IR).

C TFIISmut and the *atntr1* mutant have opposite splicing phenotypes. Heat map with scale representing the absolute difference between each respective mutant and Col-0 in alternative splice site usage. The colours represent the direction of the events as described on the axis. Each splicing event is labelled with the gene name and the type of alternative splicing event. The 3′SS/5′SS notation signifies upstream/downstream 5′/3′ splice site selection; ES marks exon skipping or exon inclusion; and IR represents intron retention or intron splicing.

PolII profiling reveals an enhanced PolII pausing at affected introns in TFIISmut

The opposite splice site selection in TFIISmut and *atntr1* is consistent with our model of NTR1-dependent transcriptional pausing at the splice sites. It also suggested that TFIIS mutation leads to enhanced PolII pausing at the splice sites. The consequence of this pausing would be manifested by the preference for upstream splice site selection in TFIISmut. To investigate this, a set of six genes was chosen. Those genes are direct targets of AtNTR1 and are oppositely spliced in *atntr1-1* and TFIISmut (5 of 6). PolII occupancy in this set of genes was investigated in TFIISmut and *atntr1-1* backgrounds. We found that TFIISmut consistently showed higher total PolII occupancy in our assay at the alternatively spliced junction (five of six genes tested) (Supplementary Fig S8). This result showed that the splicing defects observed in TFIISmut are at least correlated with increased pausing of PolII in the context of affected introns.

Previous reports indicated that aberrant splicing leads to the accumulation of PolII at introns. This paused PolII is phosphorylated at Ser5 on the CTD tail by an uncharacterised kinase in yeast (Alexander *et al*, 2010). Consequently, the phosphorylation status of the PolII CTD tail at Ser5 was analysed in *atntr1-1* and TFIISmut plants at our target genes. Indeed, the polymerase showed a predicted change in Ser5 phosphorylation that followed the changes observed in the total PolII level, suggesting that the majority of polymerase paused at those introns was Ser5-phosphorylated (Supplementary Fig S8).

Inhibiting transcription elongation by compromising PolII endonucleolytic cleavage or 6AU treatment partially reverses *atntr1* splicing defects

Next, we wanted to substantiate model in which *atntr1* splicing changes are a consequence of PolII elongation defects caused by the lack of AtNTR1. We assumed that if this model is correct, then slowing down PolII should reverse some of *atntr1* splicing defects. Analysis of splicing in *atntr1-1*TFIISmut double mutant revealed a clear but only partial reversal of *atntr1* splicing for some of the studied genes. Two of five genes studied including *DOG1* showed a shift in splice site selection towards the WT in the double mutant (Supplementary Fig S9, Supplementary Table S6). As only partial reversal at two out of five genes tested (or three out of 10 splicing isoforms changed in single mutants with P-value < 0.05 and delta $\geq 5\%$) could be observed, we extended our set to 45 splicing isoforms (in 14 different genes). Of those 45 analysed, 18 did not show any reversal in the *atntr1-1*TFIISmut double mutant compared to *atntr1-1* and 27 did show partial reversal of splicing (Supplementary Fig S9). Ten of those 27 changed events showed significant change with P-value < 0.05 and delta $\geq 5\%$ when compared directly between the *atntr1-1*TFIISmut and *atntr1-1* single mutant. TFIISmut expression analysis confirmed that the double mutant expressed our transgene at similar level to WT plants (Supplementary Fig S9C).

To further complement those observations, we have used 6AU to challenge transcription elongation in plants and analysed the alternative splicing of a selected set of genes. We have found that 6AU and MPA clearly affect splice site selection in plants. For some of the genes analysed, the pattern is opposite to pattern in *atntr1* mutant (three of six) and agree with the prediction of the kinetic coupling model (Supplementary Fig S10). What is more, analysis of *atntr1* mutant treated with 6AU showed partial or full reversal of the *atntr1* splicing defects, for events where 6AU effect in WT plants is minimal (compare column 1 and 2 in Supplementary Fig S10B). Comparison of *atntr1* and *atntr1* treated with 6AU leads to identification of 12 significantly changed splicing events. Ten of those events are partially or fully reversed in the *atntr1* 6AU-treated plants, one event changed in the same direction as in *atntr1* compared to WT and 1 event was not changed in *atntr1* compared to WT so cannot be classified (Supplementary Fig S10B, third column, events labelled with stars indicate *t*-test P-value < 0.01).

We therefore concluded that some of the splicing events altered in *atntr1* are likely to be a consequence of elongation defects and as such can be reversed by interference with PolII elongation by 6AU or inhibition of PolII endonucleolytic cleavage.

atntr1 shows low sensitivity to 6AU-mediated grow inhibition

Our data provide several lines of evidence for the role of *atntr1* in transcription elongation control at splice sites. In yeast, viability test in the presence of 6AU has been extensively used to characterise transcription elongation deficient mutants (Riles *et al*, 2004). 6AU treatment leads to reduction in *in vivo* nucleotides levels that causes transcriptional elongation to be more dependent on a fully functional RNA polymerase (Exinger & Lacroute, 1992). WT, *tfIIs* and *atntr1* mutants were subjected to the 6AU treatment. Phenotype analyses showed that *tfIIs* mutant is indeed highly sensitive to 6AU as expected from numerous reports in yeast. In contrast, *atntr1* is strongly resistant to growth inhibition by 6AU (Supplementary Fig S11). The molecular mechanism of 6AU sensitivity in plants has not been studied but the opposite sensitivity of *atntr1* and *tfIIs* mutants to 6AU is reminiscent of opposite directionality in alternative splice site selection and PolII occupancy defects. We therefore interpret the lower sensitivity of *atntr1* to 6AU as an indication of AtNTR1 negative role in transcription elongation control in plants.

Discussion

NTR1 was initially characterised as a spliceosomal disassembly factor, and substantial evidence from both humans and yeasts supports its crucial function in this process (Tsai, 2005; Yoshimoto *et al*, 2014). In *Arabidopsis*, STILP1 has been described as a NTR1 homologue required for the correct splicing of a range of targets (Jones *et al*, 2012). Here, we report that AtNTR1 (STILP1) mutants in *Arabidopsis*, in addition to circadian clock defects, show a pleiotropic phenotype, including weaker seed dormancy and a concomitant reduction in the expression of a key seed dormancy regulator, *DOG1*.

NTR1 function in splicing

In agreement with the predicted function of NTR1 in splicing, we found that *atntr1* mutants show splicing defects in a wide range of

genes, including *DOG1*, where we observe changes in alternative splicing. Although the formal role of NTR1 in spliceosomal disassembly in *Arabidopsis thaliana* remains unproven, we provide evidence for the interaction of *Arabidopsis* NTR1 with U6 snRNP, which is consistent with its function in U6 recycling in yeast and humans (Boon *et al*, 2006; Yoshimoto *et al*, 2014).

We show evidence for *in vivo,* direct interaction between AtNTR1 and GCFC domain-containing protein ILP1, in agreement with data for human homologue of NTR1. Interestingly, both *Arabidopsis* and human NTR1-interacting GCFC proteins are associated directly with gene promoters and regulate gene expression (Yoshizumi *et al*, 2006; Diao *et al*, 2012). Therefore, one possibility is that GCFC domain-containing proteins provide target specificity for NTR1 proteins. However, our data point towards strong interdependence of the NTR1 and GCFC proteins in efficient splicing, which is in disagreement with this model and suggests a role of GCFC proteins as spliceosomal factors.

Analysis of NTR1-dependent splice sites revealed that NTR1 is predominantly required for efficient splicing of strong, consensus-like, alternative splice sites. The dependence of strong alternative splice sites on NTR1 may be explained by the U1/U6 exchange defect (Konforti *et al*, 1993). It is interesting to note that the difference between NTR1-dependent and NTR1-independent splice sites lays in nucleotides forming extended interactions with U1 but not U6. Therefore, the NTR1-dependent splice sites are more efficiently bound by the U1 and may require a relatively high U6 levels or remodelling activity to exchange the U1 for the U6 RNA. Defects in NTR1 in yeast have been shown to lead to reduction in free U6 levels, providing an explanation for the NTR1 specificity we observe (Boon *et al*, 2006).

NTR1 function in PolII transcription

Beside the involvement of NTR1 in splicing, we provide several lines of evidence for additional transcription-related functions of NTR1.

Careful analysis of *atntr1* splicing defects, including splicing defects on *DOG1*, revealed a bias in alternative splice site selection that is indicative of fast PolII elongation across splice sites. AtNTR1 ChIP data showed that NTR1 is physically located at the target splice sites. Furthermore, we found that its deficiency leads not only to splicing defects but also to locally reduced PolII levels at those splice sites. This has been interpreted by us as faster transcription elongation across those sites. Several lines of evidence corroborate this interpretation. First, the localised PolII occupancy decrease would be difficult to reconcile with a transcriptional change, where PolII levels should be altered globally and not locally. Second, the opposite change in PolII occupancy and directionality of alternative splice site selection between TFIISmut and *atntr1* suggests that AtNTR1 has opposite function to TFIISmut in transcription elongation control. Consistent with this interpretation, our transgenic analyses clearly showed AtNTR1-dependent PolII accumulation on strong alternative splice sites. In addition, the reduced sensitivity of *atntr1* mutant to 6AU-mediated grow inhibition supports the putative role of NTR1 in transcription elongation control.

The directionality in alternative splice site selection observed in *atntr1-*, TFIISmut- and 6AU/MPA-treated plants is predominantly consistent with kinetic coupling of transcription and splicing (De la Mata *et al*, 2003). The kinetic coupling has to our knowledge never been shown to operate in plants. Although our data do not provide a direct confirmation of the kinetic coupling operating in plants, they are consistent with this interpretation.

Splicing analysis in *atntr1*TFIISmut double mutant showed that some of the *atntr1* splicing defects including defects observed at the *DOG1* gene can be reversed. Similar reversal of *atntr1* splicing defects was observed after *atntr1* treatment with 6AU, suggesting that this reversal can be attributed to slow transcription elongation. This can be viewed as a compensation of *bona fide* spliceosomal defects by the extension of the time window for splicing. The other possibility, that we favour, is that some of the splicing defects in *atntr1* are due to faster transcription elongation. Therefore, slowing down of the elongation rate by 6AU or interference with PolII endonucleolytic cleavage (TFIISmut) reverses those splicing defects. Our splicing assay allows for the simultaneous detection of several missplicing events of one gene. Interestingly, in the case of *DOG1* and *At4g36690*, the splice site selection event showed partial reversal in *atntr1*TFIISmut double mutant background (Supplementary Fig S9A). However, the intron retention event was fully insensitive to TFIISmut in *At4g36690* or not significantly changed in *DOG1*, even though it was altered by TFIISmut in WT backgrounds (Supplementary Fig S9A). The occurrence at the same intron of splicing events that can and cannot be reversed by TFIISmut in the *atntr1* background, even though they showed same sensitivity to TFIISmut in the WT background, suggests to us that the reversible splicing events are a consequence of elongation defects in *atntr1* rather than the spliceosome dysfunction.

In yeast, introns are sites of transient PolII pausing induced by splicing itself rather than recruitment of the spliceosome (Alexander *et al*, 2010). This pausing has been proposed to constitute a quality checkpoint for splicing, which provides feedback on transcription (Chathoth *et al*, 2014). Recently, the role of CUS2 protein as a transcriptional roadblock has been established (Chathoth *et al*, 2014). We have not addressed the role of CUS2 in transcriptional pausing in *Arabidopsis,* but our data provide evidence for an analogous role of AtNTR1. The role of NTR1 in transcription elongation control in yeast has also not been addressed. Additionally, yeast NTR1, in contrast to all other higher eukaryotes, lacks several protein domains. One interpretation is that in higher eukaryotes, the increased splicing complexity, including occurrence of alternative splicing, has led to the development of additional splicing-associated transcriptional checkpoints, including the AtNTR1 dependent.

Our chemical and genetic alteration of splicing failed to reproduce the change in PolII levels observed in the case of *atntr1* across the splice sites. Data from yeasts and humans show that herboxidiene and both tested splicing mutants work at different stages of splicing than NTR1. This together suggests that the localised reduction in PolII observed in *atntr1* is not a consequence of inefficient splicing but rather is a specific consequence of NTR1 deficiency. On the other hand, the minigene analysis showed that the NTR1-dependent PolII pausing requires a strong alternative splice site. This indicates that the strong alternative splice sites are a prerequisite for NTR1 activity both in terms of controlling splicing and in terms of controlling PolII levels at the splice sites. Our data suggest that NTR1 helps to create a pause site for elongating RNA polymerase II at alternative introns to further assist their splicing. This interpretation is consistent with the proposed role of NTR1 in quality

proofreading of splicing (Pandit *et al*, 2006; Koodathingal *et al*, 2010). Although we acknowledge that a direct assessment of PolII kinetics at the alternatively spliced exons would be required to fully validate our model, we think that a control of transcription elongation at the alternative splice sites by AtNTR1 is the most parsimonious explanation of our data. Given the involvement of H2B ubiquitin transferases homologue in *Dog1* regulation (Liu *et al*, 2007), it would be interesting to see whether it is also involved in the regulation of transcription elongation across alternative splice sites in *Arabidopsis*.

Materials and Methods

Plant materials, constructs, *Arabidopsis* transgenic lines and seed dormancy test

Wild-type Col-0 plants, *atntr1-1* (SALK_073187), *atntr1-2* (GABI_852B07), *tfIIs-2* (SALK_027259), *ilp1-1* (SALK_030650), *ilp1-2* (SALK_135563), *dog1-1* (SALK_000867) mutant alleles were used. PCR-based site-directed mutagenesis (Ho *et al*, 1989) was carried out to generate TFIISmut construct as shown in Supplementary Fig S4, under a 2,390-bp native promoter in pCambia1300. Plants were transformed as described (Logemann *et al*, 2006). NTR-GFP lines were created by the transformation (Logemann *et al*, 2006) of *atntr1-1* with ATNTR1 genomic fragment including 2,070-bp promoter cloned into pCambia1300, fused in frame with C-terminal GFP-tag. Plants were grown (Sanyo for plates or Conviron walk in chamber for soil) under controlled environmental parameters: 70% humidity, temperature 22°C and 16-h light/8-h dark photoperiod regime at 150–200 mE/m^2. For seed dormancy test, freshly harvested seeds were sterilised with 1% NaClO for 10 min and washed with distilled water three times, and seeds were then sown evenly on MS agar plate. Germination rate was scored daily until all genotypes reached 100% germination.

RNA extraction and RT–qPCR

Fourteen-day-old seedlings grown on MS plate and 16-day-old siliques were harvested, frozen in liquid nitrogen immediately and stored at −80°C. RNA was extracted by hot phenol method (Shirzadegan *et al*, 1991). RevertAid Kit (Thermo Scientific) was used for RT with 5 μg of total RNA, after DNase treatment TURBO DNA-free (Life Technologies), and oligodT primer. One microlitre of RT reaction mix was used for qPCR with SYBR Green I Master (Roche) using LightCycler 480 Instrument.

Immunoprecipitation and mass spectrometry

AtNTR1-GFP lines were used for immunoprecipitation with GFP-Trap agarose beads (Chromotek), following user manual. Eluted proteins were precipitated by acetone and digested by trypsin (Thermo Scientific). Mass spectrometry was performed in Institute of Biochemistry and Biophysics proteomics facility. Peptide mixtures were applied to RP-18 pre-column on UPLC system (NanoAcquity; Waters) using water containing 0.1% FA as a mobile phase followed by a nano-HPLC RP-18 column (75 μM; Waters) using ACN gradient (0–35% ACN in 160 min) in the presence of 0.1% FA at a flow rate of 250 nl/min. The column outlet was coupled directly to the ion source of Orbitrap Velos mass spectrometer (Thermo). The acquired MS/MS data were pre-processed with Mascot Distiller software (v. 2.4.3; MatrixScience) and a search was performed with the Mascot Search Engine (MatrixScience, Mascot Server 2.4) against the TAIR10 database (35,386 sequences; 14,482,855 residues). Mascot search settings were as follows: enzyme: trypsin, missed cleaveages: 0, fixed modifications: carbamidomethyl (C), variable modifications: oxidation (M).

Immuno-co-localisation

DNDYEGGRWEGDEFVYC and DMIDEDVEVRGGLGIGC peptides were synthesised to generate rabbit anti-AtNTR1 polyclonal antibody (Eurogentec). Immuno-co-localisation was performed as described (Zhang *et al*, 2013). Nuclei were fixed with 4% paraformaldehyde and blocked 15 min with 0.05% acBSA (Aurion, the Netherlands) in PBS buffer. Then, nuclei were incubated in double-labelling reactions with primary antibodies: anti-AtNTR1 diluted 1:200 and mouse IgG (4H8) antibody (Covance) diluted 1:100 or mouse IgG anti-SC35 (Sigma) diluted 1:100, or mouse IgM anti-RNA polymerase II H14 (recognises the phosphoserine 5 version of RNA PolII, PolIIA) or mouse IgM anti-RNA polymerase II H5 (recognises the phosphoserine 2 version of RNA PolII, PolIIO) (Covance) diluted 1:100 in PBS buffer with 0.05% ac BSA overnight at 8°C. Nuclei were then washed in PBS and incubated in secondary antibodies: Alexa Fluor 594 goat anti-rabbit (1:500, Invitrogen) and Alexa Fluor 488 goat anti-mouse IgG (1:1,000, Invitrogen) or Alexa Fluor 488 goat anti-mouse IgM (1:500; Invitrogen), at 37°C for 1 h. DNA was counterstained with 4,6-diamidino-2-phenylindole (DAPI; Fluka). The results were registered with Leica SP8 confocal and processed by Adobe PhotoShop.

BiFC assay and yeast two-hybrid assay

ORF of AtNTR1 and ILP1 were cloned to pSPYNE173 and pSPYCE (M) (Waadt *et al*, 2008), and protoplast isolation and transformation were performed as described (Wu *et al*, 2009). Fluorescence images were acquired by Nikon Eclipse TE2000-E inverted microscope and processed by Nikon EZ-C1 software. For yeast two-hybrid assay, The AtNTR1 and ILP1 ORF were amplified from cDNA and fused in frame to pGBT9 Gal4 binding domain (BD) and pGAD424 Gal4 activating domain (AD) (Clontech). The yeast strain AH109 was co-transformed with corresponding vector and grown on dropout medium –LT (leucin and trypsin deficient) for selection at 28°C. Serial decimal dilutions were used for low stringency selection on –LHT (leucin, trypsin and histidine deficient) plates and high stringency selection on –LHTA (leucin, trypsin, histidine and adenine deficient) plates.

Splicing analysis

Splicing analysis was performed using 6-FAM (Sigma-Aldrich) labelled forward primer and capillary electrophoresis on ABI3730 DNA Analyzer (Life Technologies) as described (Simpson *et al*, 2007; Raczynska *et al*, 2014). Primer sequences for alternative spliced mRNA are given in Supplementary Table S7. Peak areas for each alternative variant were analysed using PeakScanner (Life Technologies), and contribution of each alternative isoforms was calculated as

percentage of total isoforms detected. Means and standard deviations were calculated for three separate biological repetitions. Changes in AS events were considered significant if P-value < 0.05 (t-test) and change ≥ 5%. AtNTR1 splicing has been analysed using alternative splicing panel (Ji *et al*, 2007). We therefore reanalysed a selected set of 144 alternative splicing events chosen to be robust in both 2- and 3-week-old seedlings as described in figure legends. *DOG1* alternative splicing analysis shown in Supplementary Fig S1D was performed as described in Schwab (2008).

Consensus analysis

Splicing sites of affected and unaffected introns from our data set have been aligned, and Web logo was created using Weblogo3 generator (Schneider and Stephens 1990; Crooks, 2004). *Arabidopsis* consensus was created using introns from AATDB version 3-5. For AtNTR1-dependent and AtNTR1-independent intron analyses, only introns with alternative 5′ and 3′ site selection were used. Statistical significance was calculated using Fisher's two-tailed exact test based on frequencies of A/G A dinucleotides at positions +3/+4 in changed and unchanged introns with alternative splice sites (Fisher 1922).

Chemical modulation of splicing and elongation

Plant were grown in liquid culture in 1/2MS with sucrose 15 g/l, and 2-week-old plants were incubated for 3 h before harvest. 6AU (10 mg/l), MPA (5 mg/l) or herboxidiene (1.5 mg/l) were used at final concentrations shown. For 6AU viability assay, plants were grown on MS plates with 6AU (0.5 mg/l).

Chromatin immunoprecipitation (ChIP)

Chromatin immunoprecipitation was performed as described (Bowler *et al*, 2004) with IP buffer prepared as described (Kaufmann *et al*, 2010). Chromatin was sonicated at 4°C with a Diagenode Bioruptor at high intensity for 10 min (30 s on/30 s off). Antibodies: total PolII (Agrisera AS11 1804), P-Ser5 (Santa Cruz sc-47701) or peptide purified AtNTR1 antibodies described above were used with Dynabeads Protein G (Life Technologies). Chelex (Biorad) was used for de-crosslinking as described (Nelson *et al*, 2006). No antibody control was used to determine nonspecific background. Percentage of input was calculated for each sample using quantitative PCR. Primer sequences for qPCR are given in Supplementary Table S8. No antibody control showed signal an order of magnitude lower than the performed side-by-side PolII ChIP experiment (Supplementary Fig S8 bottom panel).

RNA immunoprecipitation (RIP)

Nuclear fraction was purified as for ChIP. RNA-specific steps were performed as described (Rowley *et al*, 2013). NTR1 complexes were immunoprecipitated using anti-GFP antibody (Chromotek gt-250). RNA was treated with DNase and reverse-transcribed using random primers (Thermo Scientific) and SuperScriptIII RT (Life Technologies).

Supplementary information for this article is available online: http://emboj.embopress.org

Acknowledgements

We thank Professor John Brown and Dr Craig Simpson for help with alternative splicing panel, Thomas R. Webb for his excellent advice with selecting splicing modulator and Zbigniew Pietras for critical reading of the manuscript. This project was supported by National Science Centre (N N301 388239 and N N301 269237 to SS, UMO-2011/01/M/NZ2/01435 to AJ, UMO-2011/03/N/NZ2/03070 and UMO-2014/12/T/NZ2/00246 to JD), National Centre for Research and Development (LIDER/22/139/L-1/09/NCBiR/2010 to SS and YG) and Foundation for Polish Science (TEAM2010-5/9 to SS and GB and MPD/2010/7 for JD).

Author contributions

JD performed splicing platform analysis, PolII ChIPs, RIP; AK, DS and YG performed the immunolocalisation; GB performed Y2H; YG obtained the TFIISmut plants and performed all other experiments; YG, JD, AJ and SŚ designed the experiments; AJ and SŚ analysed the data; and SŚ wrote the paper.

Conflict of interest

The authors declare that they have no conflict of interest.

References

Agafonov DE, Deckert J, Wolf E, Odenwälder P, Bessonov S, Will CL, Urlaub H, Lührmann R (2011) Semiquantitative proteomic analysis of the human spliceosome via a novel two-dimensional gel electrophoresis method. *Mol Cell Biol* 31: 2667 – 2682

Alexander RD, Innocente SA, Barrass JD, Beggs JD (2010) Splicing-dependent RNA polymerase pausing in yeast. *Mol Cell* 40: 582 – 593

Batsché E, Yaniv M, Muchardt C (2005) The human SWI/SNF subunit Brm is a regulator of alternative splicing. *Nat Struct Mol Biol* 13: 22 – 29

Bentsink L, Jowett J, Hanhart CJ, Koornneef M (2006) Cloning of DOG1, a quantitative trait locus controlling seed dormancy in *Arabidopsis*. *Proc Natl Acad Sci USA* 103: 17042 – 17047

Boon K-L, Auchynnikava T, Edwalds-Gilbert G, Barrass JD, Droop AP, Dez C, Beggs JD (2006) Yeast Ntr1/Spp382 mediates Prp43 function in postspliceosomes. *Mol Cell Biol* 26: 6016 – 6023

Bowler C, Benvenuto G, Laflamme P, Molino D, Probst AV, Tariq M, Paszkowski J (2004) Chromatin techniques for plant cells. *Plant J* 39: 776 – 789

Braberg H, Jin H, Moehle EA, Chan YA, Wang S, Shales M, Benschop JJ, Morris JH, Qiu C, Hu F, Tang LK, Fraser JS, Holstege FCP, Hieter P, Guthrie C, Kaplan CD, Krogan NJ (2013) From structure to systems: high-resolution, quantitative genetic analysis of RNA polymerase II. *Cell* 154: 775 – 788

Brody Y, Neufeld N, Bieberstein N, Causse SZ, Böhnlein E-M, Neugebauer KM, Darzacq X, Shav-Tal Y (2011) The in vivo kinetics of RNA polymerase II elongation during co-transcriptional splicing. *PLoS Biol* 9: e1000573

Buratowski S (2009) Progression through the RNA Polymerase II CTD Cycle. *Mol Cell* 36: 541 – 546

Chanarat S, Seizl M, Strässer K (2011) The Prp19 complex is a novel transcription elongation factor required for TREX occupancy at transcribed genes. *Genes Dev* 25: 1147 – 1158

Chathoth KT, Barrass JD, Webb S, Beggs JD (2014) A splicing-dependent transcriptional checkpoint associated with prespliceosome formation. *Mol Cell* 53: 779 – 790

Cheung ACM, Cramer P (2011) Structural basis of RNA polymerase II backtracking, arrest and reactivation. *Nature* 471: 249 – 253

Close P, East P, Dirac-Svejstrup AB, Hartmann H, Heron M, Maslen S, Chariot A, Söding J, Skehel M, Svejstrup JQ (2012) DBIRD complex integrates alternative mRNA splicing with RNA polymerase II transcript elongation. *Nature* 484: 386 – 389

Crooks GE (2004) WebLogo: a sequence logo generator. *Genome Res* 14: 1188 – 1190

Cvitkovic I, Jurica MS (2013) Spliceosome database: a tool for tracking components of the spliceosome. *Nucleic Acids Res* 41: D132 – D141

De la Mata M, Alonso CR, Kadener S, Fededa JP, Blaustein M, Pelisch F, Cramer P, Bentley D, Kornblihtt AR (2003) A slow RNA polymerase II affects alternative splicing in vivo. *Mol Cell* 12: 525 – 532

De la Mata M, Muñoz MJ, Alló M, Fededa JP, Schor IE, Kornblihtt AR (2011) RNA polymerase II elongation at the crossroads of transcription and alternative splicing. *Genet Res Int* 2011: 1 – 9

Diao Y, Guo X, Li Y, Sun K, Lu L, Jiang L, Fu X, Zhu H, Sun H, Wang H, Wu Z (2012) Pax3/7BP Is a Pax7- and Pax3-binding protein that regulates the proliferation of muscle precursor cells by an epigenetic mechanism. *Cell Stem Cell* 11: 231 – 241

Dujardin G, Lafaille C, de la Mata M, Marasco LE, Muñoz MJ, Le Jossic-Corcos C, Corcos L, Kornblihtt AR (2014) How slow RNA polymerase II elongation favors alternative exon skipping. *Mol Cell* 54: 683 – 690

Dutertre M, Sanchez G, De Cian M-C, Barbier J, Dardenne E, Gratadou L, Dujardin G, Le Jossic-Corcos C, Corcos L, Auboeuf D (2010) Cotranscriptional exon skipping in the genotoxic stress response. *Nat Struct Mol Biol* 17: 1358 – 1366

Exinger F, Lacroute F (1992) 6-Azauracil inhibition of GTP biosynthesis in *Saccharomyces cerevisiae*. *Curr Genet* 22: 9 – 11

Filichkin SA, Priest HD, Givan SA, Shen R, Bryant DW, Fox SE, Wong W-K, Mockler TC (2009) Genome-wide mapping of alternative splicing in *Arabidopsis thaliana*. *Genome Res* 20: 45 – 58

Fisher RA (1922) On the interpretation of $\chi 2$ from contingency tables, and the calculation of P. *J R Stat Soc* 85: 87 – 94

Grasser M, Kane CM, Merkle T, Melzer M, Emmersen J, Grasser KD (2009) Transcript elongation factor TFIIS is involved in *Arabidopsis* seed dormancy. *J Mol Biol* 386: 598 – 611

Hasegawa M, Miura T, Kuzuya K, Inoue A, Won Ki S, Horinouchi S, Yoshida T, Kunoh T, Koseki K, Mino K, Sasaki R, Yoshida M, Mizukami T (2011) Identification of SAP155 as the Target of GEX1A (Herboxidiene), an Antitumor Natural Product. *ACS Chem Biol* 6: 229 – 233

Ho SN, Hunt HD, Horton RM, Pullen JK, Pease LR (1989) Site-directed mutagenesis by overlap extension using the polymerase chain reaction. *Gene* 77: 51 – 59

Howe KJ, Kane CM, Ares M Jr (2003) Perturbation of transcription elongation influences the fidelity of internal exon inclusion in *Saccharomyces cerevisiae*. *RNA* 9: 993 – 1006

Ip JY, Schmidt D, Pan Q, Ramani AK, Fraser AG, Odom DT, Blencowe BJ (2011) Global impact of RNA polymerase II elongation inhibition on alternative splicing regulation. *Genome Res* 21: 390 – 401

Izban MG, Luse DS (1992) The RNA polymerase II ternary complex cleaves the nascent transcript in a 3′–5′ direction in the presence of elongation factor SII. *Genes Dev* 6: 1342 – 1356

Ji Q, Huang C-H, Peng J, Hashmi S, Ye T, Chen Y (2007) Characterization of STIP, a multi-domain nuclear protein, highly conserved in metazoans, and essential for embryogenesis in *Caenorhabditis elegans*. *Exp Cell Res* 313: 1460 – 1472

Jones MA, Williams BA, McNicol J, Simpson CG, Brown JWS, Harmer SL (2012) Mutation of *Arabidopsis* SPLICEOSOMAL TIMEKEEPER LOCUS1 causes circadian clock defects. *Plant Cell* 24: 4066 – 4082

Kaida D, Motoyoshi H, Tashiro E, Nojima T, Hagiwara M, Ishigami K, Watanabe H, Kitahara T, Yoshida T, Nakajima H, Tani T, Horinouchi S, Yoshida M (2007) Spliceostatin A targets SF3b and inhibits both splicing and nuclear retention of pre-mRNA. *Nat Chem Biol* 3: 576 – 583

Kaufmann K, Muiño JM, Østerås M, Farinelli L, Krajewski P, Angenent GC (2010) Chromatin immunoprecipitation (ChIP) of plant transcription factors followed by sequencing (ChIP-SEQ) or hybridization to whole genome arrays (ChIP-CHIP). *Nat Protoc* 5: 457 – 472

Komarnitsky P (2000) Different phosphorylated forms of RNA polymerase II and associated mRNA processing factors during transcription. *Genes Dev* 14: 2452 – 2460

Konforti BB, Koziolkiewicz MJ, Konarska MM (1993) Disruption of base pairing between the 5′ splice site and the 5′ end of U1 snRNA is required for spliceosome assembly. *Cell* 75: 863 – 873

Koodathingal P, Novak T, Piccirilli JA, Staley JP (2010) The DEAH box ATPases Prp16 and Prp43 cooperate to proofread 5′ splice site cleavage during pre-mRNA splicing. *Mol Cell* 39: 385 – 395

Lagisetti C, Yermolina MV, Sharma LK, Palacios G, Prigaro BJ, Webb TR (2014) Pre-mRNA splicing-modulatory pharmacophores: the total synthesis of herboxidiene, a pladienolide-herboxidiene hybrid analog and related derivatives. *ACS Chem Biol* 9: 643 – 648

Liu Y, Koornneef M, Soppe WJJ (2007) The absence of histone H2B monoubiquitination in the *Arabidopsis* hub1 (rdo4) mutant reveals a role for chromatin remodeling in seed dormancy. *Plant Cell* 19: 433 – 444

Logemann E, Birkenbihl RP, Ulker B, Somssich IE (2006) An improved method for preparing Agrobacterium cells that simplifies the *Arabidopsis* transformation protocol. *Plant Methods* 2: 16

Marquez Y, Brown JWS, Simpson C, Barta A, Kalyna M (2012) Transcriptome survey reveals increased complexity of the alternative splicing landscape in *Arabidopsis*. *Genome Res* 22: 1184 – 1195

Mayas RM, Maita H, Semlow DR, Staley JP (2010) Spliceosome discards intermediates via the DEAH box ATPase Prp43p. *Proc Natl Acad Sci* 107: 10020

Miller-Wideman M, Makkar N, Tran M, Isaac B, Biest N, Stonard R (1992) Herboxidiene, a new herbicidal substance from *Streptomyces chromofuscus* A7847. Taxonomy, fermentation, isolation, physico-chemical and biological properties. *J Antibiot (Tokyo)* 45: 914 – 921

Mortensen SA, Grasser KD (2014) The seed dormancy defect of *Arabidopsis* mutants lacking the transcript elongation factor TFIIS is caused by reduced expression of the DOG1 gene. *FEBS Lett* 588: 47 – 51

Nelson JD, Denisenko O, Bomsztyk K (2006) Protocol for the fast chromatin immunoprecipitation (ChIP) method. *Nat Protoc* 1: 179 – 185

Pagani F, Stuani C, Zuccato E, Kornblihtt AR, Baralle FE (2003) Promoter architecture modulates CFTR exon 9 skipping. *J Biol Chem* 278: 1511 – 1517

Palusa SG, Ali GS, Reddy ASN (2007) Alternative splicing of pre-mRNAs of *Arabidopsis* serine/arginine-rich proteins: regulation by hormones and stresses: stress regulation of alternative splicing of SR genes. *Plant J* 49: 1091 – 1107

Pan Q, Shai O, Lee LJ, Frey BJ, Blencowe BJ (2008) Deep surveying of alternative splicing complexity in the human transcriptome by high-throughput sequencing. *Nat Genet* 40: 1413 – 1415

Pandit S, Lynn B, Rymond BC (2006) Inhibition of a spliceosome turnover pathway suppresses splicing defects. *Proc Natl Acad Sci* 103: 13700 – 13705

Raczynska KD, Stepien A, Kierzkowski D, Kalak M, Bajczyk M, McNicol J, Simpson CG, Szweykowska-Kulinska Z, Brown JWS, Jarmolowski A (2014)

The SERRATE protein is involved in alternative splicing in *Arabidopsis thaliana*. *Nucleic Acids Res* 42: 1224 – 1244

Reines D (1992) Elongation factor-dependent transcript shortening by template-engaged RNA polymerase II. *J Biol Chem* 267: 3795 – 3800

Riles L, Shaw RJ, Johnston M, Reines D (2004) Large-scale screening of yeast mutants for sensitivity to the IMP dehydrogenase inhibitor 6-azauracil. *Yeast* 21: 241 – 248

Rowley MJ, Böhmdorfer G, Wierzbicki AT (2013) Analysis of long non-coding RNAs produced by a specialized RNA polymerase in *Arabidopsis thaliana*. *Methods (San Diego Calif)* 63: 160 – 169

Saint-André V, Batsché E, Rachez C, Muchardt C (2011) Histone H3 lysine 9 trimethylation and HP1γ favor inclusion of alternative exons. *Nat Struct Mol Biol* 18: 337 – 344

Schwab M (2008) Identification of novel seed dormancy mutants in *Arabidopsis thaliana* and molecular and biochemical characterization of the seed dormancy gene *DOG1*. PhD Thesis, Faculty of Mathematics and Natural Sciences, University of Cologne, Cologne

Schneider TD, Stephens RM (1990) Sequence logos: a new way to display consensus sequences. *Nucleic Acids Res* 18: 6097 – 6100

Sekimizu K, Kobayashi N, Mizuno D, Natori S (1976) Purification of a factor from Ehrlich ascites tumor cells specifically stimulating RNA polymerase II. *Biochemistry (Mosc)* 15: 5064 – 5070

Shirzadegan M, Christie P, Seemann JR (1991) An efficient method for isolation of RNA from tissue cultured plant cells. *Nucleic Acids Res* 19: 6055

Shukla S, Kavak E, Gregory M, Imashimizu M, Shutinoski B, Kashlev M, Oberdoerffer P, Sandberg R, Oberdoerffer S (2011) CTCF-promoted RNA polymerase II pausing links DNA methylation to splicing. *Nature* 479: 74 – 79

Sigurdsson S, Dirac-Svejstrup AB, Svejstrup JQ (2010) Evidence that transcript cleavage is essential for RNA polymerase II transcription and cell viability. *Mol Cell* 38: 202 – 210

Simpson CG, Fuller J, Maronova M, Kalyna M, Davidson D, McNicol J, Barta A, Brown JWS (2007) Monitoring changes in alternative precursor messenger RNA splicing in multiple gene transcripts. *Plant J* 53: 1035 – 1048

Swaraz AM, Park Y-D, Hur Y (2011) Knock-out mutations of *Arabidopsis* SmD3-b induce pleotropic phenotypes through altered transcript splicing. *Plant Sci. Int J Exp Plant Biol* 180: 661 – 671

Tannukit S, Wen X, Wang H, Paine ML (2008) TFIP11, CCNL1 and EWSR1 protein-protein interactions, and their nuclear localization. *Int J Mol Sci* 9: 1504 – 1514

Tsai R-T (2005) Spliceosome disassembly catalyzed by Prp43 and its associated components Ntr1 and Ntr2. *Genes Dev* 19: 2991 – 3003

Waadt R, Schmidt LK, Lohse M, Hashimoto K, Bock R, Kudla J (2008) Multicolor bimolecular fluorescence complementation reveals simultaneous formation of alternative CBL/CIPK complexes in planta. *Plant J Cell Mol Biol* 56: 505 – 516

Wahl MC, Will CL, Lührmann R (2009) The spliceosome: design principles of a dynamic RNP machine. *Cell* 136: 701 – 718

Wen X, Lei Y-P, Zhou YL, Okamoto CT, Snead ML, Paine ML (2005) Structural organization and cellular localization of tuftelin-interacting protein 11 (TFIP11). *Cell Mol Life Sci* 62: 1038 – 1046

Wu F-H, Shen S-C, Lee L-Y, Lee S-H, Chan M-T, Lin C-S (2009) Tape-*Arabidopsis* sandwich—a simpler *Arabidopsis* protoplast isolation method. *Plant Methods* 5: 16

Yoshimoto R, Okawa K, Yoshida M, Ohno M, Kataoka N (2014) Identification of a novel component C2ORF3 in the lariat-intron complex: lack of C2ORF3 interferes with pre-mRNA splicing via intron turnover pathway. *Genes Cells* 19: 78 – 87

Yoshizumi T, Tsumoto Y, Takiguchi T, Nagata N, Yamamoto YY, Kawashima M, Ichikawa T, Nakazawa M, Yamamoto N, Matsui M (2006) Increased level of polyploidy 1, a conserved repressor of CYCLINA2 transcription, controls endoreduplication in *Arabidopsis*. *Plant Cell* 18: 2452 – 2468

Zhang C-J, Zhou J-X, Liu J, Ma Z-Y, Zhang S-W, Dou K, Huang H-W, Cai T, Liu R, Zhu J-K, He X-J (2013) The splicing machinery promotes RNA-directed DNA methylation and transcriptional silencing in *Arabidopsis*. *EMBO J* 32: 1128 – 1140

